

## LONG-TERM *IN VIVO* REGENERATION OF PERIPHERAL NERVES THROUGH BIOENGINEERED NERVE GRAFTS

P. G. DI SUMMA,<sup>a,b</sup> D. F. KALBERMATTEN,<sup>a,c</sup>  
E. PRALONG,<sup>d</sup> W. RAFFOUL,<sup>a</sup> P. J. KINGHAM<sup>b,e,\*</sup>  
AND G. TERENGI<sup>b</sup>

<sup>a</sup>Department of Plastic, Reconstructive and Aesthetic Surgery, University Hospital of Lausanne, Switzerland

<sup>b</sup>Blond McIndoe Research Laboratories, Regenerative Biomedicine Group, The University of Manchester, Manchester, UK

<sup>c</sup>Department of Plastic, Reconstructive and Aesthetic Surgery, University Hospital of Basel, Switzerland

<sup>d</sup>Department of Neurosurgery, University Hospital of Lausanne, Switzerland

<sup>e</sup>Department of Integrative Medical Biology, Section of Anatomy, Umeå University, Umeå, Sweden

**Abstract**—Although autologous nerve graft is still the first choice strategy in nerve reconstruction, it has the severe disadvantage of the sacrifice of a functional nerve. Cell transplantation in a bioartificial conduit is an alternative strategy to improve nerve regeneration. Nerve fibrin conduits were seeded with various cell types: primary Schwann cells (SC), SC-like differentiated bone marrow-derived mesenchymal stem cells (dMSC), SC-like differentiated adipose-derived stem cells (dASC). Two further control groups were fibrin conduits without cells and autografts. Conduits were used to bridge a 1 cm rat sciatic nerve gap in a long term experiment (16 weeks). Functional and morphological properties of regenerated nerves were investigated. A reduction in muscle atrophy was observed in the autograft and in all cell-seeded groups, when compared with the empty fibrin conduits. SC showed significant improvement in axon myelination and average fiber diameter of the regenerated nerves. dASC were the most effective cell population in terms of improvement of axonal and fiber diameter, evoked potentials at the level of the gastrocnemius muscle and regeneration of motoneurons, similar to the autografts. Given these results and other advantages of adipose derived stem cells such as ease of harvest and relative abundance, dASC could be a clinically translatable route towards new methods to enhance peripheral nerve repair. © 2011 IBRO. Published by Elsevier Ltd. All rights reserved.

**Key words:** adipose-derived stem cells, fibrin conduit, nerve repair, Schwann cell.

Peripheral nerve injuries can affect up to 5% of patients that are admitted to a level 1 trauma centre (Belkas et al.,

\*Correspondence to: P. J. Kingham, Department of Integrative Medical Biology, Section of Anatomy, Umeå University, SE-90187 Umeå, Sweden. Tel: +46-90-786-9754; fax: +46-90-786-5480.

E-mail address: paul.kingham@anatomy.umu.se (P. J. Kingham).

**Abbreviations:** AD, axonal diameter; ASC, adipose-derived stem cell; CMAP, compound muscle action potential; dASC, Schwann cell-like differentiated adipose-derived stem cell; dMSC, Schwann cell-like differentiated bone marrow-derived mesenchymal stem cell; FBS, foetal bovine serum; FD, fiber diameter; GFAP, glial fibrillary acidic protein; MSC, mesenchymal stem cell; MT, myelin thickness; SC, Schwann cell.

0306-4522/11 \$ - see front matter © 2011 IBRO. Published by Elsevier Ltd. All rights reserved.  
doi:10.1016/j.neuroscience.2011.02.052

2004; Taylor et al., 2008). These injuries represent an important issue in medicine as patients with peripheral nerve trauma are often at the peak of their employment productivity and any loss or decrease of function is particularly devastating (Whitlock et al., 2009). Driven by enormous clinical need, interest in peripheral nerve regeneration has become a prime focus of research and an area of growth within the field of tissue engineering.

In clinical practice, ideal repair of a nerve injury is to perform an end-to-end coaptation of proximal and distal stumps to achieve a tension-free repair. If the loss of tissue precludes this type of repair, autologous donor nerves are currently the gold standard to bridge peripheral defects. However, autograft harvest requires a second operative site with the sacrifice of a functional nerve, resulting in donor sensory loss, potential formation of neuroma and neuropathic pain (Pfister et al., 2007; Zhang et al., 2010). This dictates research towards the development of tissue engineered alternatives: nerve conduits are tubular structures designed to bridge the gap of a sectioned nerve, protect the nerve from scar formation and guide the regenerating fibers into the distal nerve stump (Mohanna et al., 2005; Pfister et al., 2007). A number of attempts have been made to develop conduits made of synthetic or biodegradable materials (Belkas et al., 2004), which could guide the regenerating axons without inhibiting the process of growth and maturation. To date, none of them can be considered an effective clinical alternative to the autograft.

For these reasons, researchers have focused on improving bioengineered scaffolds by recreating features of the permissive environment present in the peripheral nervous system (PNS) after injury. The regenerative potential present in the PNS is thought to be due to the interplay between growth factors, cellular elements (Schwann cells), their basal lamina and the extracellular matrix proteins (Ide, 1996; Hall, 1997; Chalfoun et al., 2006). Schwann cells (SC) and their basal lamina represent the key component of nerve regeneration, as they serve as scaffolds for the regenerating axons, which grow through the empty basal lamina tubes. Proliferating SC also produce many neurotrophic factors (Terenghi, 1995; Mirsky et al., 2002) which can improve peripheral regeneration *in vivo* (Guenard et al., 1992; Mosahebi et al., 2001; Rodriguez et al., 2005). SC however have limited clinical applications since the culture of an adequate quantity of cells to achieve optimal conditions for transplantation in nerve conduits is time consuming and requires particular care for *in vitro* expansion and a constant input of growth factors (Pereira Lopes et al., 2006). Moreover, SC are not easily accessible without nerve biopsy and bear the need to sacrifice an autologous nerve, with the related complications of

anesthesia and pain at the harvest site (di Summa et al., 2010; Erba et al., 2010). With the growing applicability of stem cells in all avenues of medicine, new opportunities have become available for the treatment for degenerative and traumatic nerve injuries (Barry and Murphy, 2004; Gardner, 2007).

Adult stem cells (Sanchez-Ramos et al., 2000; Kokai et al., 2005) show ability to differentiate into neuro-progenitor type cells. Bone marrow-derived mesenchymal stem cells (MSCs) can be induced to differentiate into non-mesenchymal fates *in vitro*, such as Schwann cells (Dezawa et al., 2001; Caddick et al., 2006), improving myelin formation and nerve regeneration *in vivo* after their transplantation into different models of peripheral nerve injury (Tohill et al., 2004a; Keilhoff et al., 2006). In the last few years, adipose tissue has been indicated as a novel and promising source of multipotent cells (adipose-derived stem cells, ASC), which can be differentiated towards mesenchymal and non-mesenchymal lineages, similar to bone-marrow stromal cells (Zuk et al., 2001, 2002; Tholpady et al., 2003; Strem et al., 2005). Moreover, ASC can be easily isolated in large quantities and expanded *in vitro* (Kingham et al., 2007; Matsumoto et al., 2008) and, in terms of clinical use, they may be harvested by conventional liposuction procedure under local anaesthesia, with considerably lower donor site morbidity when compared with bone marrow aspiration.

Since the first reports of induction of ASC into a neuronal phenotype (Safford et al., 2002; Zuk et al., 2002), there have been a number of studies showing expression of mature neuronal and glial markers (Ashjian et al., 2003; Kang et al., 2004; Safford et al., 2004; Guilak et al., 2006) as we recently reviewed (Erba et al., 2010). Our group showed how ASC could be differentiated towards a Schwann cell-like phenotype, expressing markers like S-100, glial fibrillary acidic protein (GFAP) and P75 neurotrophin receptor and enhancing neurite outgrowth in an *in vitro* co-culture model (Kingham et al., 2007). Recently, we discovered expression of myelin proteins P0 and peripheral myelin protein 22 after differentiation of both ASC and MSC (Mantovani et al., 2010). We confirmed the neurotrophic potential shown *in vitro* from differentiated adipose-derived stem cells (dASC) with a brief term *in vivo* study (di Summa et al., 2010). Bioresorbable nerve guides made by fibrin glue (Kalbermatten et al., 2009) were seeded with different types of regenerative cells including primary Schwann cells and SC-like differentiated mesenchymal and adipose-derived stem cells. After sciatic nerve axotomy, the conduits were implanted and the nerves were left to regenerate across a 1 cm gap for 2 weeks. The groups in which the conduit was combined with the cells showed enhanced axonal regeneration and Schwann cell migration when compared with the empty fibrin conduit, and dASC displayed similar potency as differentiated MSC (dMSC) (di Summa et al., 2010). The aim of this current study was to determine whether these encouraging results could translate to long-term benefits for nerve repair. We present a 4-month study using fibrin conduits seeded with various cell types and control autografts to repair a 1-cm rat sciatic nerve gap. Histological analysis, retrograde mo-

toneuron labelling, electrophysiology and evaluation of muscle atrophy are described.

## EXPERIMENTAL PROCEDURES

### Experimental animals

All animal protocols were approved by the local veterinary commission in Lausanne, Switzerland and were carried out in accordance with the European Community Council directive 86/609/ECC for the care and use of laboratory animals. Male Sprague–Dawley rats (Janvier, France) weighing 250 g were used for this study.

### Cell cultures and differentiation

All cells were obtained from Sprague–Dawley rats (Janvier, France). Schwann cells were isolated from sciatic nerves as previously described (di Summa et al., 2010) and maintained in Dulbecco's Modified Eagle's Medium plus Glutamax (DMEM, Invitrogen, UK) containing 10% foetal bovine serum (FBS), 1% penicillin-streptomycin and supplemented with 14  $\mu$ M forskolin and 126 ng/ml neuregulin.

ASC were harvested as described previously (Kingham et al., 2007) and maintained in Modified Eagle Medium ( $\alpha$ -MEM; Invitrogen, UK) containing 10% (v/v) FBS, and 1% (v/v) penicillin/streptomycin solution.

MSC were harvested from adult Sprague–Dawley rat femoral bones as previously described (Caddick et al., 2006; di Summa et al., 2010) and maintained in the same growth medium as for ASC.

Undifferentiated ASC and MSC were differentiated at early passages. Growth medium was removed from sub-confluent cultures and replaced with medium supplemented with 1 mM  $\beta$ -mercaptoethanol (Sigma-Aldrich, UK) for 24 h. Cells were then washed and fresh medium supplemented with 35 ng/ml all-trans-retinoic acid was added. A further 72 h later, cells were washed and medium replaced with differentiation medium; cell growth medium supplemented with 5 ng/ml platelet-derived growth factor (PDGF; PeproTech Ltd., UK), 10 ng/ml basic fibroblast growth factor (bFGF; PeproTech Ltd., UK), 14  $\mu$ M forskolin and 40 ng/ml of recombinant neuregulin- $\beta$ 1 (NRG1- $\beta$ 1, R&D Systems, UK). Cells were incubated for 2 weeks under these conditions with fresh medium added approximately every 72 h. In order to confirm the effectiveness of the differentiation of stem cells and their similarity to the Schwann cell population, we performed cell immunostaining for typical Schwann cells markers S100 and GFAP as previously described (Caddick et al., 2006; Kingham et al., 2007). The percentage of double positive cells were as follows: Schwann cells 97.4 $\pm$ 2.1%, bone marrow MSC 61.8 $\pm$ 5.2% and ASC 42.74 $\pm$ 8.4%.

### Fibrin conduit preparation

The fibrin conduit was prepared from two compound fibrin glue (Tisseel® Kit VH 1.0, Baxter SA, USA) as previously described (di Summa et al., 2010). Fibrin glue was dispensed in a silicone prepared mould around a stainless steel core and pressed into shape for 5 min. This allows the generation of uniform conduits measuring 14 mm in length, with a 2 mm lumen and 1 mm wall thickness designed to bridge a 10 mm gap in the left sciatic nerve of 250 g adult Sprague–Dawley rats.

### Experimental design and surgical procedure

Five experimental groups were included: fibrin conduit without cells (empty), fibrin conduit seeded with primary adult SC, fibrin conduit seeded with dMSC, fibrin conduit seeded with dASC and a control group composed by autografts. All groups (each one formed by five animals for a total  $n=25$ ) were left in place for 16

weeks and subsequently conduits were harvested together with the proximal and distal nerve stumps.

A few hours before implantation in the rats, cells were trypsinized and after centrifugation,  $2 \times 10^6$  cells were suspended in 50  $\mu\text{l}$  of growth medium and injected into the fibrin tubes. To avoid cell dispersion during the procedure, one side of the fibrin tube was capped by a fibrin glue clot as we previously reported (di Summa et al., 2010). Before implantation, the fibrin conduit was easily decapped from the fibrin clots at its ends. The fibrin tubes without cells contained just growth medium. The operation was performed on the left sciatic nerve under aseptic conditions using a power focus surgical microscope (Carl Zeiss, Germany). A skin incision from the left knee to the hip was made for exposure of the underlying muscles, which were then retracted to reveal the sciatic nerve (di Summa et al., 2010). The sciatic nerve was transected and nerve ends were fixed to the conduit by a single epineurial suture (9/0 Prolene, Ethicon, Germany); proximal and distal nerve stumps were inserted 2 mm into the tube thus leaving a 10 mm gap. In the autograft group, after meticulous dissection of the sciatic nerve, a 1 cm segment was excised, reversed and resutured on each side by two epineurial sutures (Pettersson et al., 2010). Muscles and fascia layers were closed with single resorbable stitches (4/0 Softcat, Braun, Germany) and the skin by a continuous running suture (4/0 Prolene, Ethicon, Germany). All experimental groups were housed on sawdust, one animal/cage with a 12 h light:12 h dark cycle (lights on at 06.00 h) and received food and water *ad libitum*.

### Electrophysiology

Fifteen weeks after implantation of nerve conduits, animals were anesthetized with isoflurane (Attane™, Minrad, USA) and the regenerated sciatic nerve was exposed under a dissecting microscope as outlined above.

Electromyographic analysis was carried out by stimulating both proximally (S1) and distally (S2) to the regenerated nerve (unresorbed prolene sutures were taken as referral points) with a monopolar cathodic electrode (Prass Standard Monopolar Stimulator, Xomed®, Medtronic, Jacksonville, USA), the anode being positioned on the rat tail. Stimulations were increased to the supramaximal level (square negative pulse, 1 Hz; 0.2-ms pulse duration; 1 mA) in order to elicit compound evoked muscle action potentials (CMAP). CMAP reproducibility was visually determined by four consecutive stimulations that were averaged for CMAP delays and amplitudes measurement (deflection from zero from peak-to-peak). Muscle contractions were recorded by paired subdermal electrodes placed into the gastrocnemius muscle of the left limb. Recordings were made using a Micromed System 98 EMG (Micromed, Treviso, Italy) equipment and the signal was filtered between 10 and 1000 Hz.

### Retrograde neuronal labelling

In order to identify spinal motoneurons which had regenerated through the neural conduit, a fluorescent dye was injected distally to the distal suture to retrogradely trace neurons in the spinal cord. 15 weeks after implantation, but 6 days before explantation, the surgical site was reopened under isoflurane general anesthesia (Attane™, MinRad, USA) and 5  $\mu\text{l}$  of a 4% Fast Blue solution (FB, EMS-Chemie GmbH, Germany) was injected into the sciatic nerve 5 mm distal to the implant as previously described (Fine et al., 2002). After labelling, the nerve was rinsed in normal saline to avoid any non-specific labelling and the wound was closed in layers. Animals were left to survive six further days in order to enable labelling of the neurons.

### Tissue harvesting and processing

*Regenerated sciatic nerves.* After 16 weeks of conduit implantation, the animals were deeply anaesthetized with an i.p.

injection of a mixture 1:5 of ketamine (Ketalar, Parke-Davis; 75 mg  $\text{kg}^{-1}$ ) and xylazine (Rompun, Bayer; 10 mg  $\text{kg}^{-1}$ ). The regenerated left sciatic nerves were harvested under operating microscope together with proximal and distal stump. Nerve samples were fixed in 4% paraformaldehyde in PBS for 2–4 h and then washed and stored in 0.2 g glycine in 100 ml PBS prior to embedding. On the day of embedding, after a further PBS wash, nerves were immersed for 2 h in 2% osmium tetroxide (Sigma, St. Louis, MO, USA) in the same PBS solution. The nerves were then dehydrated by an increasing alcohol series starting from 30% ethanol. The specimens were then embedded in paraffin and serial cross sections (5- $\mu\text{m}$  thick) were cut using a rotary Ultramicrotome (Leica Microsystems, Wetzlar, Germany). Cross sections of nerves were conducted starting 1 mm distally to the distal prolene suture (where the distal stump had been originally sutured to the conduit) in order to allow visualization of regenerated fibers entering the distal nerve stump. Slides were either stained with Masson's trichrome according to an established protocol (Di Scipio et al., 2008) or directly mounted in DPX (Fluka) after dehydration with ascending ethanol passages.

*Gastrocnemius muscles.* Using the operating microscope, both left and right (control) gastrocnemius muscles were carefully cleaned and dissected out, dividing their tendinous origin and insertion from the bone. Muscles were weighed following harvest. In each rat, the gastrocnemius muscle weight ratio (experimental/control, E/C) was calculated based on the weight of the gastrocnemius muscle on the experimental leg (left leg) versus the control leg (right leg) according to the following formula:

$$E/C = \text{weight experimental} / \text{weight control muscle}$$

*Spinal cords.* After nerve and muscle harvesting the animals were administered an i.p. overdose of sodium pentobarbital (Somnasol, Butler Animal Health Supply, Dublin, OH, USA; 240 mg  $\text{kg}^{-1}$ ) and perfused transcardially with a cold 0.9% saline solution, followed by 4% paraformaldehyde in PBS (pH=7.4). The spinal cord segments L4–L6 were harvested and post fixed overnight in 4% paraformaldehyde at 4 °C. Spinal cords were then cryoprotected in 30% sucrose for 48 h at 4 °C, embedded in OCT freezing media (Tissue-tek, Sakura, Japan) and stored at –80 °C. Serial longitudinal 50- $\mu\text{m}$  thick sections were cut using a cryomicrotome (Leica instruments, Germany) and mounted on slides (Superfrost® plus, Menzel-Gläser, Germany). Slides were then washed for 15 min in PBS, followed by a final wash in nanopure water and left to dry overnight in the dark. The following day, after 3 min dehydration in toluene, the slides were cover-slipped with DPX and examined under fluorescence microscope (Olympus BX40, Olympus America Inc., USA).

### Retrograde labelled motoneurons count

Nuclear profiles of labelled motoneurons were counted in all sections at 250 $\times$  final magnification with a fluorescence microscope (Olympus BX40, Olympus America Inc., USA). Since uniformity was noticed in nuclear size and since the nuclear diameters were small in comparison to the section thickness (Jacob, 1998), the total number of nuclear profiles was not corrected for split nuclei according to previous experience (Pettersson et al., 2010).

### Histomorphometry and image analysis

5  $\mu\text{m}$ -thick distal cross sections of regenerated nerves of different experimental groups were examined by light microscopy at a final magnification of 400 $\times$ . Automatic, real-time pattern matching, mosaic images were taken in order to reconstruct the whole nerve cross area at high definition (MosaicPro, Explora Nova Laboratory Imaging, Bordeaux, France). For the morphometric analysis of the sciatic nerve, five representative fields covering at least 20% of the nerve cross-sectional area were selected. Samples were

given a code to conceal their identity and then five random fields were selected in the central body and superior, inferior, left and right lateral thirds of the sample. At least 500 fibers were analysed per animal: the cross section area, the number of myelinated fibers (n), myelin thickness (MT), average axonal diameter (AD) and fiber diameter (FD) were assessed using Image ProPlus Imaging software version 4.5 (Media Cybernetics, Marlow, UK). From the above mentioned measurements were obtained the g-ratio (AD/FD) and the fiber density, calculated as number of fibers/mm<sup>2</sup>. The axonal area ( $\pi AD/2^2$ ) and the fiber area ( $\pi FD/2^2$ ) were obtained assuming the circularity of the nerve fiber area (Wang et al., 2010). The myelinated area was considered as the difference between fiber area and axonal area. Once all analysis was complete the samples were decoded and mean $\pm$ SEM calculated for each group.

### Data and statistical analysis

One-way analysis of variance (ANOVA) with Bonferroni multiple comparison test was used to statistically analyse data (GraphPad Prism 5.00, San Diego, USA). Distribution of axonal and fiber diameters were analysed using Stata version 9.1 (StataCorp LP, College Station, USA); percentages were compared by Bonferroni multiple comparison test. Significance was determined as \*  $P < 0.05$ , \*\*  $P < 0.01$ , \*\*\*  $P < 0.001$ .

## RESULTS

### Post-operative complications and autotomy

All animals survived the surgical procedure and recovered from anaesthesia. One animal from the fibrin+SC group developed a postoperative subcutaneous hematoma at the surgical site which was evacuated with no consequences. No other surgical complications occurred except autotomy of the foot following sciatic nerve axotomy. Major autotomy of the experimental foot (considered as complete loss or damage to multiple phalanges and/or presence of open wounds), which lead to premature euthanasia of the animals, was detected in three animals out of 25 (12%: two animals from the dMSC group, one animal from the SC group), and always developed within the first month after nerve axotomy. New animals to re-establish the n number/group, substituted these animals.

### In vivo electrophysiological analysis

Fifteen weeks post implantation of the conduit and 6 days before euthanasia, the surgical site of the left (experimental) sciatic nerve was reopened under aseptic conditions and the electrical properties of the regenerated nerves were tested *in vivo*. Before CMAP recording, all nerves were tested for viability using the following methods. Tibial and peroneal branches distal to the regenerated gap were briefly stimulated to assess muscle specific movements (plantar flexion for the tibial nerve and foot eversion for the peroneal). Contraction of the gluteal muscles and consequent movement of the paw was considered as a proof of nerve viability (Whitlock et al., 2009) and successful regeneration across the gap. All rats of all examined groups (empty fibrin conduit, dMSC, dASC, SC and autograft) showed successful muscle contraction. After assessment of nerve viability, CMAP were recorded and four electromyographic waves were averaged in each rat (Fig. 1). The

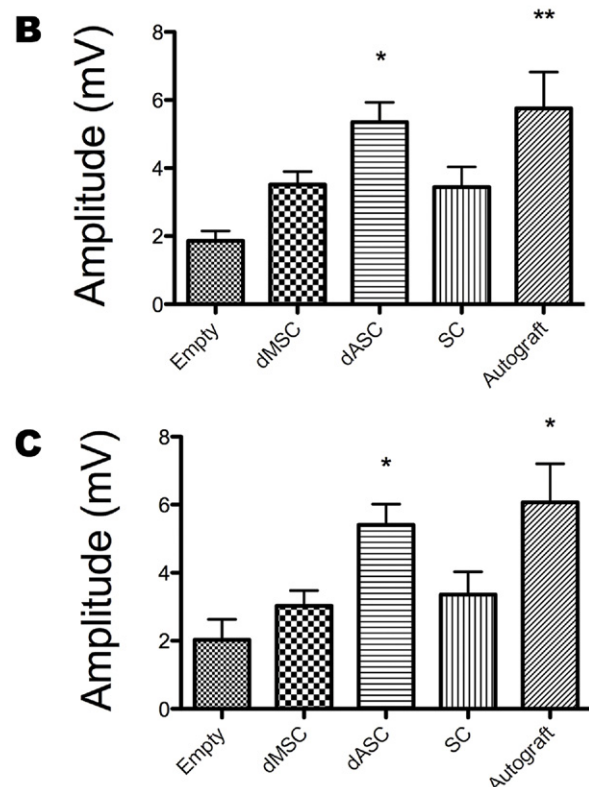
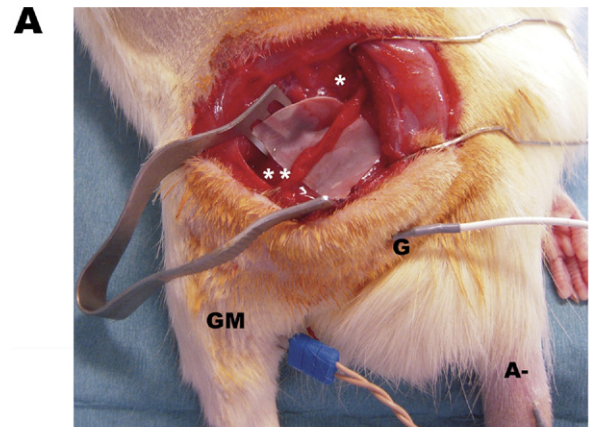


**Fig. 1.** The electrophysiology set-up (A), with visualization of proximal (\*) and distal (\*\*) stimulation site, recording electrode at the level of gastrocnemius muscle (GM), anode placed subdermally at the level of the tail (A-), ground (G). Graphs showing the mean amplitudes of compound muscle action potential (CMAP) after stimulation of the sciatic nerve with a monopolar cathodic electrode both proximally (B) and distally (C) to the regenerated segment. Values shown are mean $\pm$ SEM, significance is referred to the empty fibrin conduit group: \*  $P < 0.05$ , \*\*  $P < 0.01$ . For interpretation of the references to color in this figure legend, the reader is referred to the Web version of this article.

monopolar cathodic electrode was set on 1 mA and the regenerated nerves were stimulated proximally (S1). The experiment was repeated distally (S2) to the point where the conduit had been sutured in order to assess efficient conductivity without dispersion.

CMAP in the autograft group and in the group of fibrin conduit seeded with dASC, showed significantly higher

**Fig. 2.** Regenerated nerve 16 wks after implantation *in situ* (A) and after harvesting (B). Graph showing mean number of counted motoneurons and significant differences referred to the empty fibrin conduit group (C). Fast blue labelled spinal motoneurons 16 wks following total sciatic nerve axotomy repaired by simple empty fibrin conduit, fibrin conduit seeded with SC-like differentiated MSC (dMSC), SC-like differentiated ASC (dASC), primary Schwann cells (SC) and autografts (columns from left to right). Scale bar: 50  $\mu\text{m}$ ; values shown are expressed as mean  $\pm$  SEM, significance is referred to the empty fibrin conduit group: \*  $P < 0.05$ , \*\*  $P < 0.01$ . For interpretation of the references to color in this figure legend, the reader is referred to the Web version of this article.

amplitudes when compared with the empty fibrin conduit group (\*\* Autograft  $5.75 \text{ mV} \pm 1.067$ ; \* dASC  $5.35 \text{ mV} \pm 0.58$  vs. empty  $1.86 \text{ mV} \pm 0.29$ ). In the groups where fibrin conduits were seeded with dMSC and SC, recorded values were almost double the amplitudes recorded in the empty fibrin group (dMSC  $3.51 \text{ mV} \pm 0.378$ ; SC  $3.44 \text{ mV} \pm 0.59$ ) (Fig. 1B), but did not reach significance. No statistical difference was present when comparing the other experimental groups between themselves. When considering CMAP that followed the stimulation in S2, distally to the regenerated nerve, we could observe a pattern of amplitudes which almost overlapped the pattern seen after proximal stimulations (Fig. 1C). These measurements confirmed the absence of signal dispersion and the good conductivity of new nerves. As proximally, the au-

tograft group and the group of fibrin seeded with dASC generated wave potentials significantly higher when compared to the empty fibrin conduit group (respectively: empty  $2.03 \text{ mV} \pm 0.60$ ; dMSC  $3.03 \text{ mV} \pm 0.45$ ; \* dASC  $5.41 \text{ mV} \pm 0.61$ ; SC  $3.36 \text{ mV} \pm 0.67$ ; \* autograft  $6.07 \text{ mV} \pm 1.13$ ).

#### Harvesting of regenerated nerves

At 4 months post implantation, conduits and autografts were explanted (Fig. 2). Fibrin was found to be totally resorbed and in all groups the proximal and distal stumps could be easily identified. Partial adherences of the regenerated nerve to the surrounding muscular tissue were removed by minimal blunt dissection under an operating microscope. No evidence of site infection, scar tissue or signs of neuroma were found.

### Quantification of labelled motor neurons

The number of motoneurons extending axons through the neural guides was evaluated by counting Fast-Blue traced neurons. All spinal cords showed presence of retrogradely traced neurons, confirming the crossing of the gap and the viability of the regenerated nerves (Fig. 2).

In the autograft group, 16 weeks following total left sciatic axotomy and nerve grafting,  $990 \pm 45$  (mean  $\pm$  SEM) spinal motoneurons had regenerated across the 1 cm gap. These results were found to be significantly higher when compared with the empty fibrin conduit group which showed only  $452 \pm 41$  regenerated motoneurons (\*\*  $P < 0.01$ ). All fibrin conduits seeded with cells showed higher number of regenerated motoneurons when compared with the empty fibrin conduit group (Fig. 2C). Although all cell groups showed a strong positive trend, just the group in which the fibrin conduit was seeded with dASC, showed a significantly higher count of neurons, approaching the numbers of the autografts (F+dMSC  $757 \pm 96$ ; \* F+dASC  $921 \pm 68$ ; F+SC  $786 \pm 126$ , all expressed as mean  $\pm$  SEM).

### Wet muscle mass

A total transection of the sciatic nerve produces the loss of the neural innervation to the gastrocnemius muscle, which leads to a decrease in the muscle mass (Fig. 3A). This decline in muscle mass was quantified in this study by

weighing the excised gastrocnemius muscle and calculating a ratio of muscle mass, based on the mass of the experimental muscle vs. the mass of the muscle in the control side (referred as E/C). As the E/C ratio approaches 1, less muscle atrophy is present. The highest E/C ratio was displayed by the autograft group, which was significantly higher when compared with the empty fibrin conduit group (\*\*\*) Autograft  $0.51 \pm 0.03$  vs. F empty  $0.34 \pm 0.014$ , all expressed as mean  $\pm$  SEM). When the fibrin conduit was coupled with regenerative cells, they showed a protective effect against muscle atrophy, with significantly higher muscle mass when compared to the fibrin conduit alone (respectively: \* F+dMSC  $0.432 \pm 0.013$ ; \* F+dASC  $0.437 \pm 0.03$ ; F+SC  $0.453 \pm 0.02$  all expressed as mean  $\pm$  SEM) (Fig. 3B). No significant differences were found when the groups which received the cells were compared to the autograft. All the experimental groups were also expressed as a percentage of the gold standard control (autograft), reaching over 85% of the gastrocnemius muscle mass of the autografts when cells were seeded into the fibrin conduits (F empty  $66.43\% \pm 2.826$ ; \* F+dMSC  $84.60\% \pm 2.620$ ; \* F+dASC  $85.45\% \pm 5.628$ ; \* F+SC  $88.67\% \pm 3.242$ , all expressed as mean  $\pm$  SEM).

### Histological and morphometric analysis

Examination by light microscopy of cross sections through the distal part of the regenerated nerves was conducted

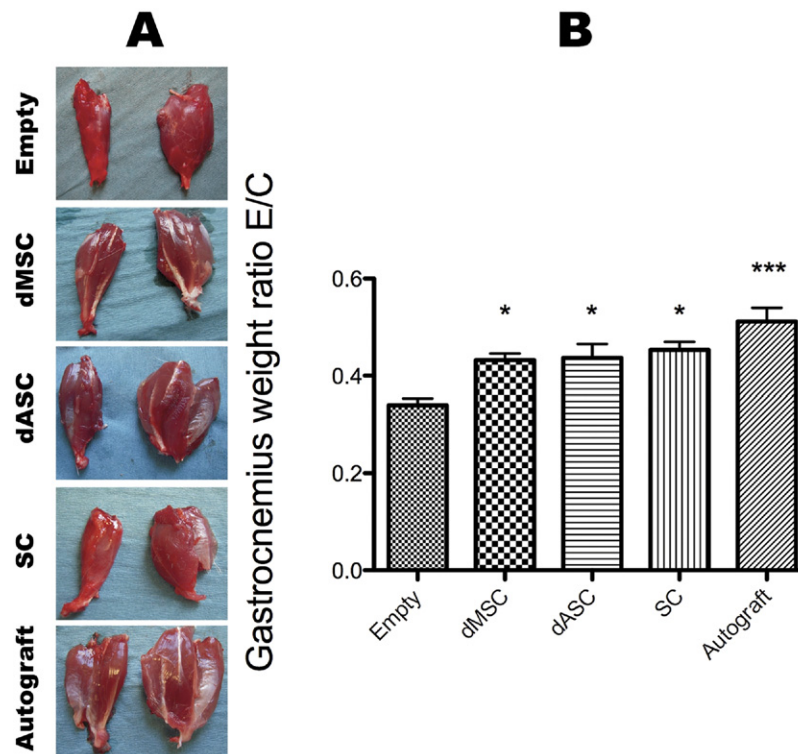


**Fig. 3.** The evaluation of muscle atrophy 16 wks after total axotomy (experimental muscles on the left and contralateral on the right) and repair by simple empty fibrin conduit treatment, fibrin conduit seeded with SC-like differentiated MSC (dMSC), SC-like differentiated ASC (dASC), primary Schwann cells (SC) and autografts (A, from top to bottom). Graph showing mean gastrocnemius muscle weight ratio (experimental/control, E/C) and statistically significant differences among the groups (B). Values shown are expressed as mean  $\pm$  SEM, significance is referred to the empty fibrin conduit group: \*  $P < 0.05$ , \*\*\*  $P < 0.001$ . For interpretation of the references to color in this figure legend, the reader is referred to the Web version of this article.

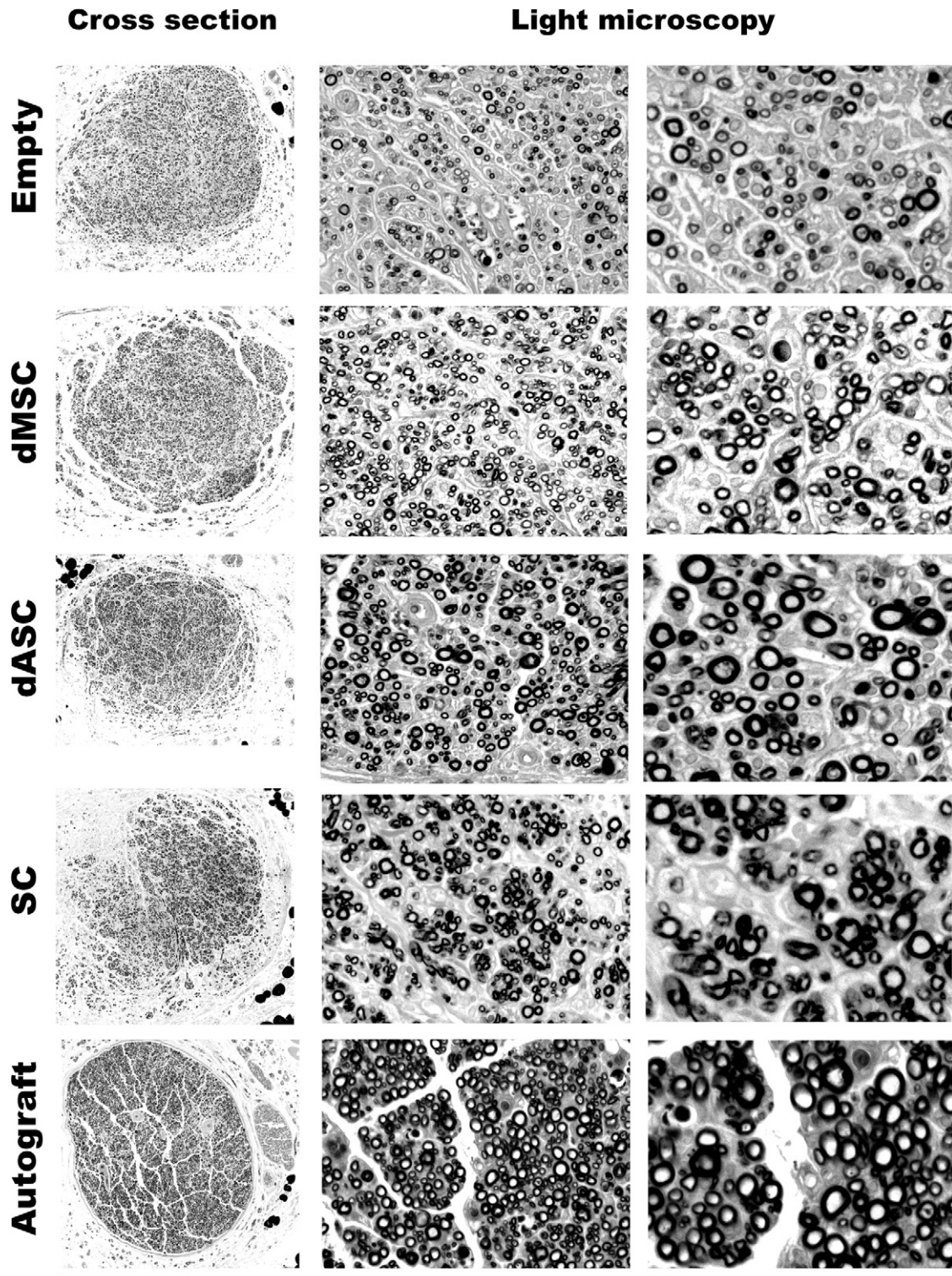


**Fig. 4.** Evaluation of sciatic nerve regeneration 16 wks after total axotomy with simple empty fibrin conduit treatment, fibrin conduit seeded with SC-like differentiated MSC (dMSC), SC-like differentiated ASC (dASC), primary Schwann cells (SC) and autografts (rows from top to bottom). Columns from left to right: the general appearance of whole nerve cross sections (scale bar: 500  $\mu\text{m}$ ), light microscopy representative pictures of myelinated axons in the distal stump, 1 mm distal to the suture site (scale bars: 10 and 20  $\mu\text{m}$ ).

(Fig. 4). Whole nerve cross sectional areas were compared between the groups, showing no statistical differ-

ences between them. However, autograft and F+dASC groups showed a tendency towards a bigger cross sec-

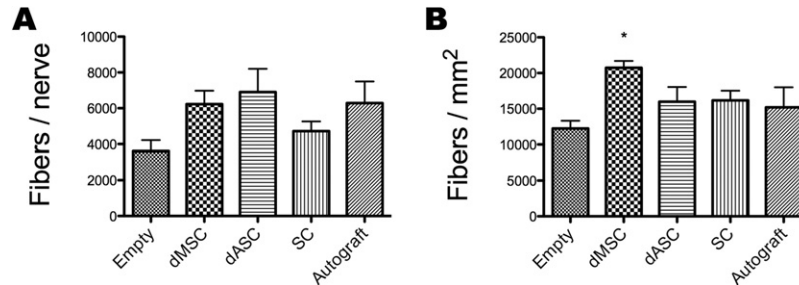


**Fig. 5.** Graphs showing total number of fibers in the distal nerve stump (A) and average fiber density (B) 16 wks after total axotomy and repair by simple empty fibrin conduit treatment, fibrin conduit seeded with SC-like differentiated MSC (dMSC), SC-like differentiated ASC (dASC), primary Schwann cells (SC) and autografts. Values shown are expressed as mean  $\pm$  SEM, significance is referred to the empty fibrin conduit group: \*  $P < 0.05$ .

tional area when compared to the empty fibrin conduit ( $P = 0.52$  and  $P = 0.209$  respectively). Endoneurial architecture was conserved but myelinated axons were not always enclosed in fascicles. The average number of myelinated axons entering the distal stump ranged from  $3616 \pm 604$  in the empty fibrin conduit group to  $6902 \pm 1300$  in the F+dASC group (Fig. 5A). However, no differences were statistically evident across the experimental groups (Table 1). When considering the differences in terms of cross sectional area among the groups, the fiber density (n fibers/nerve surface) gives a more correct estimation of the number of regenerating fibers. Lowest fiber density was found in the empty fibrin conduit group ( $12,230 \pm 1091$  fibers/mm<sup>2</sup>), which was significantly inferior when compared to the F+dMSC group ( $20,733 \pm 962$  fibers/mm<sup>2</sup>, \*  $P < 0.05$ ) (Fig. 5B). No other statistical difference emerged when comparing the other groups. When analyzing morphological differences, average myelin thickness in autograft and F+SC groups, resulted in significantly higher values when they were compared to the empty fibrin tube (autograft \*\*\*  $P < 0.01$ ; \* F+SC  $P < 0.05$ ) (Fig. 6A). No statistical difference was noticed when the empty guide was compared to the fibrin conduit seeded with dMSC ( $P = 1$ ) or dASC ( $P = 0.058$ ) (Table 1). The myelinated surface was significantly improved in autograft and F+dASC groups when compared to the empty conduit (autograft \*\*  $P < 0.01$ ; \* F+dASC  $P < 0.05$ ). The SC group did not reach a statistically significant difference in myelinated surface, suggesting how this measure is influenced by the

axonal diameter (Fig. 6B). Average axonal diameters (Fig. 7A) of autograft and F+dASC were significantly improved when compared to the empty fibrin conduit group (\*  $P < 0.05$ ). F+dMSC and F+SC showed a positive trend in improving axon diameter without reaching a statistical significance. Average fiber diameter estimations were obtained by adding to the average AD the measured average value of myelin thickness times 2 (MT $\times$ 2). Group analysis confirmed, as expected, the trend seen in AD, confirming a significantly superior fiber diameter in the autograft and F+dASC groups when compared to the empty fibrin conduit (\*\*  $P < 0.01$ , Fig. 7B). F+SC group showed improved average fiber diameter in absolute values but did not reach significance, F+dMSC group displayed a significantly smaller FD when compared to the autograft group ( $P < 0.05$ ). The axonal and fiber diameter distribution curves highlighted the skew towards greater sizes with the addition of cells to the conduits or treatment with autograft (Fig. 7A, B).

Using the previously obtained average axon and fiber diameter, we were able to calculate average axonal ( $\pi AD/2$ )<sup>2</sup> and fiber ( $\pi FD/2$ )<sup>2</sup> area among the different groups, by assuming the cross-sectioned fibers as circles as shown in previous publications (Piquilloud et al., 2007; Wang et al., 2010). Average fiber area in the autograft and F+dASC group was found to be almost double the value encountered in the empty fibrin group (respectively: empty fibrin  $8.413 \pm 0.8043$   $\mu\text{m}^2$ ; autograft  $16.57 \pm 1.742$   $\mu\text{m}^2$  \*\*  $P < 0.01$ ; \* F+dASC  $15.58 \pm 1.956$   $\mu\text{m}^2$  \*  $P < 0.05$ ). More-

**Table 1.** Morphometric analysis of the distal nerve stump

	Fibrin empty	F+dMSC	F+dASC	F+SC	Autograft
MT ( $\mu\text{m}$ ) $\pm$ SEM	0.703 $\pm$ 0.033	0.787 $\pm$ 0.0196	0.899 $\pm$ 0.037	0.917 $\pm$ 0.055*	1.032 $\pm$ 0.060***##
AD ( $\mu\text{m}$ ) $\pm$ SEM	1.634 $\pm$ 0.109	1.838 $\pm$ 0.077	2.266 $\pm$ 0.172*	1.873 $\pm$ 0.090	2.238 $\pm$ 0.118*
FD ( $\mu\text{m}$ ) $\pm$ SEM	3.049 $\pm$ 0.151	3.412 $\pm$ 0.0667	4.081 $\pm$ 0.226**	3.751 $\pm$ 0.157	4.302 $\pm$ 0.226***
G-ratio (AD/FD) $\pm$ SEM	0.524 $\pm$ 0.019	0.527 $\pm$ 0.0140	0.551 $\pm$ 0.0144	0.499 $\pm$ 0.020	0.5100 $\pm$ 0.008
Axonal area ( $\mu\text{m}^2$ ) $\pm$ SEM	2.613 $\pm$ 0.351	3.212 $\pm$ 0.241	5.176 $\pm$ 0.799*	3.522 $\pm$ 0.371	4.854 $\pm$ 0.502
Fiber area ( $\mu\text{m}^2$ ) $\pm$ SEM	8.413 $\pm$ 0.804	10.27 $\pm$ 0.356	15.58 $\pm$ 1.956*	12.42 $\pm$ 1.144	16.57 $\pm$ 1.742***
Myelinated area ( $\mu\text{m}^2$ ) $\pm$ SEM	5.750 $\pm$ 0.549	7.056 $\pm$ 0.217	10.41 $\pm$ 1.204*	8.898 $\pm$ 0.886	11.72 $\pm$ 1.273***
Fiber density (n/mm <sup>2</sup> ) $\pm$ SEM	12,230 $\pm$ 1091	20,733 $\pm$ 962*	15,984 $\pm$ 2072	16,184 $\pm$ 1350	15,200 $\pm$ 2805
Total fiber count $\pm$ SEM	3616 $\pm$ 604	6231 $\pm$ 751	6902 $\pm$ 1300	4724 $\pm$ 542	6286 $\pm$ 1210
Nerve cross area (mm <sup>2</sup> ) $\pm$ SEM	0.299 $\pm$ 0.052	0.296 $\pm$ 0.026	0.436 $\pm$ 0.033	0.307 $\pm$ 0.0434	0.423 $\pm$ 0.0420

Significance values denoted with the \* symbol compare samples with the empty fibrin conduit group (\*  $P < 0.05$ , \*\*  $P < 0.01$ , \*\*\*  $P < 0.001$ ). Significance values denoted with # symbol compare samples with the fibrin+dMSC group (#  $P < 0.05$ , ##  $P < 0.01$ ).

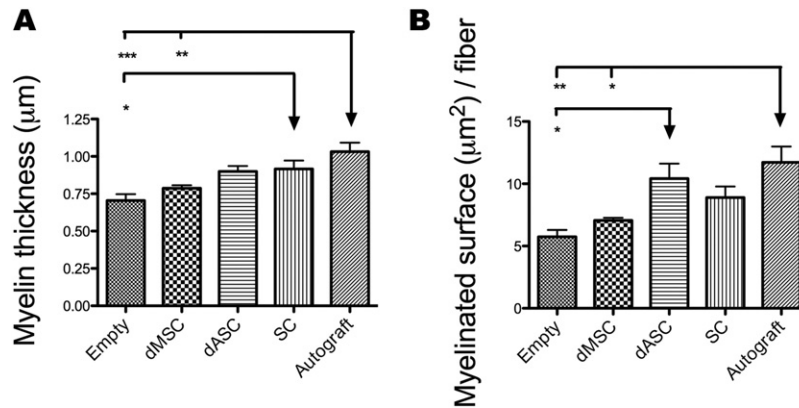


**Fig. 6.** Graphs showing average myelin thickness (A) and average myelinated surface in the fibers (B) 16 wks after total axotomy and repair by simple empty fibrin conduit treatment, fibrin conduit seeded with SC-like differentiated MSC (dMSC), SC-like differentiated ASC (dASC), primary Schwann cells (SC) and autografts. Values shown are expressed as mean  $\pm$  SEM, statistically significant differences among the groups are shown by connecting arrows: \*  $P < 0.05$ , \*\*  $P < 0.01$ , \*\*\*  $P < 0.001$ .

over, the autograft group resulted in a significantly higher fiber surface when compared to the F+dMSC group ( $P < 0.05$ ) (see Table 1 for further details). Myelinated area was also calculated as the difference between fiber and axonal areas, showing a similar pattern to the one of fiber area (Fig. 6B). Finally, as a structural index of optimal axonal myelination, the g-ratio (inner axonal diameter/outer axonal diameter, AD/FD) was calculated. No statistically significant differences in g-ratio values were identified among all groups (Table 1).

## DISCUSSION

Successful crossing of a nerve gap depends on the formation of a new extracellular matrix scaffold, over which blood vessels, fibroblasts and Schwann cells can migrate and progress towards the distal nerve stump (Rodriguez et al., 2000). Indeed, surviving axons from the proximal stump will develop growth cones and extend along the connective strands bridging the gap. Unless axonal contact is re-established in a timely fashion, however, this growth supportive environment is not maintained (Walsh and Midha, 2009). In longer defects, this may imply a failure of the nerve regeneration process because the nerve stumps are unable to provide in time a proper cable where regenerative elements can migrate and create a permissive environment to nerve regeneration (Belkas et al., 2004). Transplantation of SC (Guenard et al., 1992; Tohill et al., 2004b; Rodriguez et al., 2005) and bone marrow mesenchymal stem cells (Dezawa et al., 2001; Tohill et al., 2004a; Keilhoff et al., 2006) into nerve guides has been shown to provide proper support for regenerating axons, improving fiber regeneration and remyelination.

Few publications are available on the long term effect of ASC in nerve regeneration. In this study we chose 4 months as a time-point for analysis of the effect of cells on regeneration—this is consistent with previous publications describing different evaluation techniques for peripheral nerve repair (Vleggeert-Lankamp, 2007). Santiago et al. showed survival of undifferentiated human adipose precursor

cells up to 12 weeks after transplantation with a favourable effect on muscle atrophy. A modest decrease in muscle atrophy was attributed to the cells that did not show any spontaneous differentiation when in contact to the niche at the injury site (Santiago et al., 2009). More recently, neuronally differentiated adipose-derived stem cells, have been successfully transplanted in a constructed acellular nerve matrix derived from a porcine intercostal nerve, with a significant increment in nerve regeneration at 3 months, when compared to the constructed graft alone (Zhang et al., 2010). Currently to the best of our knowledge, SC-like differentiated ASC have never been tested in a long term experiment within a bioartificial nerve conduit.

Fibrin is one of the extracellular matrix components which serves as a natural growth terrain for regenerating axons following nerve injury (Chen et al., 2007). Previous works have shown its reliability as a matrix for stem cells transplantation (Bensaid et al., 2003; Kalbermatten et al., 2008) or for local delivery of neurotrophic factors (Jubran and Widenfalk, 2003). A biodegradable tubular nerve conduit made of fibrin was shown to be an effective device, ensuring axonal guidance and supporting long term neuronal regeneration (Kalbermatten et al., 2009; Pettersson et al., 2010). In our experience, fibrin exhibited key properties of a neural guide (Chalfoun et al., 2006) such as simplicity of implantation, biodegradability, absence of scarring or inflammatory reaction and efficient guidance of axonal fibers. Fibers were able to cross a 1 cm sciatic nerve gap, showing effective regeneration in both morphological (histology, muscle weight ratio) and functional (electrophysiology, retrograde labelling of motoneurons) investigations. However, besides confirming the reliability of the fibrin conduit as a nerve guide in long term experiments (Pettersson et al., 2010), the present report demonstrates that combining the fibrin conduit with primary SC and SC-like differentiated adult stem cells (dMSC and dASC), could improve fibrin conduit performances in the long term. Moreover, dASC seemed to be the most effective cell line when compared to dMSC and even SC.

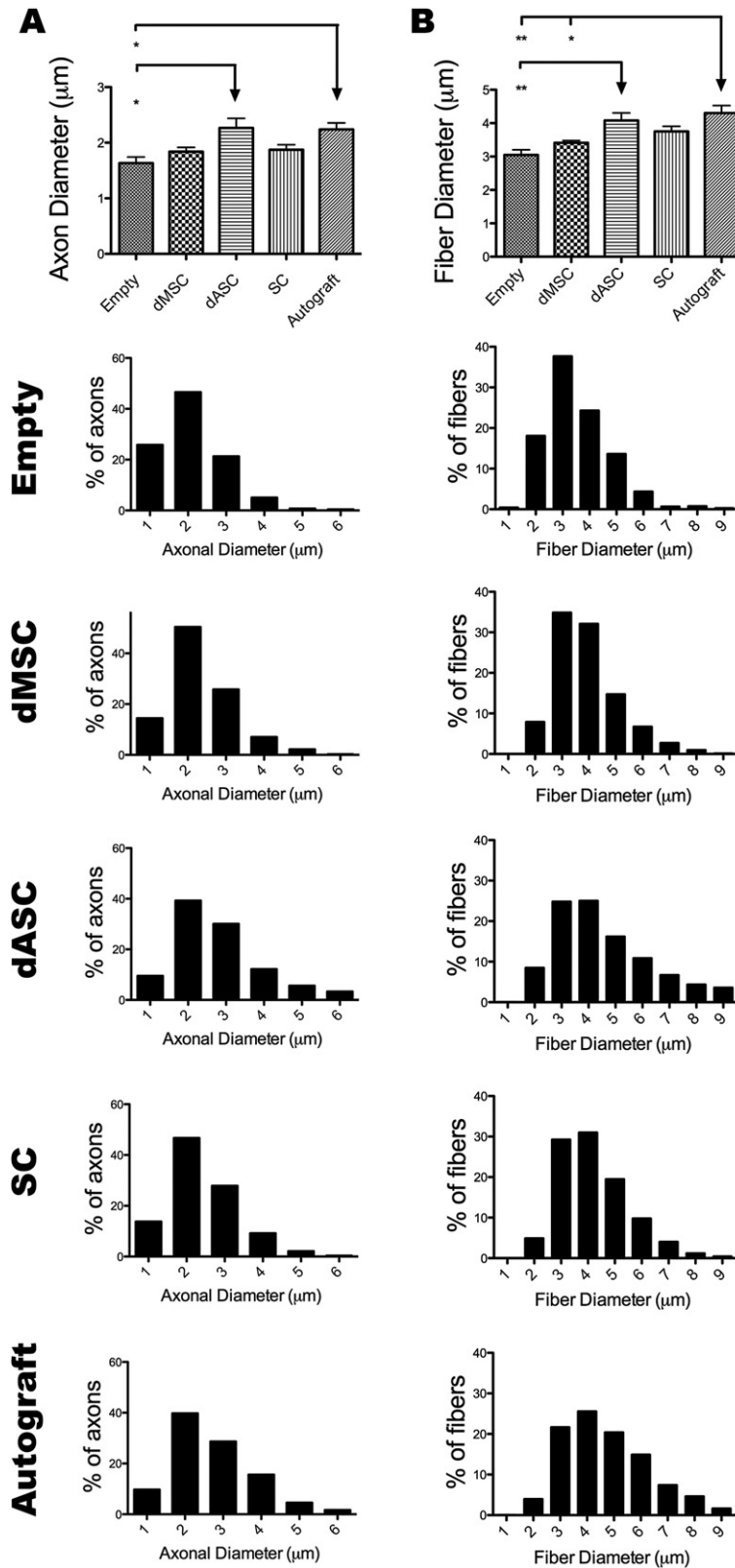


**Fig. 7.** Axonal (left column) and fiber (right column) analysis 16 wks after total axotomy and repair by simple empty fibrin conduit treatment, fibrin conduit seeded with SC-like differentiated MSC (dMSC), SC-like differentiated ASC (dASC), primary Schwann cells (SC) and autografts. Left column: graph showing average axonal diameter (A) in different experimental groups; from top to bottom, average percentage distribution of axonal diameter of each group. Right column: graph showing average fiber diameter (B) in different experimental groups; from top to bottom, average percentage distribution of fiber diameter in each group. Values shown are expressed as mean $\pm$ SEM, statistically significant differences among the groups are shown by connecting arrows: \*  $P < 0.05$ , \*\*  $P < 0.01$ .

Fifteen weeks after conduit implantation, in order to evaluate the degree of reinnervation, we performed *in vivo* measurements of CMAP at the gastrocnemius muscle, after stimulation proximally and distally to the regenerated nerve. CMAPs were recognized to have a resolving power when evaluating nerve regeneration and electrical functionality of the grafted or regenerated nerves (Vleggeert-Lankamp, 2007). All animals in all groups showed electrical viability of the nerves, but differences in recorded amplitudes were present among the groups. Amplitude reductions are mainly due to axonal loss or presence of smaller calibre axons, but may be also influenced by demyelination when this leads to temporal dispersion or partial distal conduction blocks (Johnsen and Fuglsang-Fredriksen, 2000; Tankisi et al., 2007). CMAPs after proximal stimulation of the sciatic nerve were significantly increased in the autograft group and in the group of fibrin seeded with dASC. This result reflects the morphometric analysis, where these two groups showed a significant improved axon and fiber diameter when compared to the empty fibrin group. Even if the SC group showed a significantly thicker myelin sheet when compared to the empty fibrin conduit (Fig. 6A, B), they did not reach a significant superiority in terms of axonal diameter ( $P=1$ ) or fiber diameter ( $P=0.1$ ). This may explain the lower CMAPs despite the good axonal myelination. In the group where fibrin was seeded with dMSC, wave amplitudes were similar to the SC group, consistent to the average diameter size between the two groups. When CMAPs were recorded after stimulation distal to the regenerated nerve, absolute values were generally conserved (see results section for details), with maintained relationships among the groups. This confirms that, even with differences between different groups, the gap was crossed by functional fibers, with no blocks or anomalies in conductivity.

The origin of the regenerated fibers was identified by retrograde labelling in order to assess eventual differences in motoneuron regeneration capacities among the groups. Consistently, the same groups which had displayed the best muscle potentials in the electrophysiological tests (autograft and fibrin+dASC groups), showed a significantly higher number of regenerated motoneurons when compared to the empty fibrin conduit group. Even if observing a positive trend in motoneuron count in the SC and dMSC groups, we were not able to find a significant statistical difference when these groups compared to the empty fibrin conduit group ( $P=0.172$  and  $P=0.276$ , respectively). Similar to previous reports (Pettersson et al., 2010), the number of labelled motoneurons is not necessarily correlated to the total distal fiber count. Indeed, in regenerating nerves, fibers will branch at the time of lesion towards the distal stump, including collateral branching and misdirected growth that may simultaneously reach different target organs (Rodriguez et al., 2000; Vleggeert-Lankamp, 2007) and will successively incur the pruning process (Brushart, 1993). As a result, when considering together electrophysiological findings and retrograde labelled count of motoneurons, it seem that, closely to the autograft, dASC allowed the formation of a higher number

of neurons signalling to a motor unit, improving functional contraction and CMAPs when compared to the empty fibrin conduit.

Relative muscle weight ratio, defined as the ratio of the gastrocnemius muscle weight from the experimental side to that of the control side (E/C), is an indirect way to estimate sciatic nerve regeneration. In our study, the three groups seeded with regenerative cells (SC, dMSC, dASC), manifested a significant improvement of wet muscle mass when compared to the empty fibrin conduit group, almost approaching 90% of the values encountered in the autograft group. However, no differences were evident among the three groups. In a previous report, undifferentiated human adipose precursor cells, seemed to reduce muscular atrophy after a sciatic nerve lesion in rats by improving the size of muscle fibers (Santiago et al., 2009). Nevertheless, the gastrocnemius muscle weight ratio did not vary significantly, appearing less sensitive than the myofibers/area ratio. Taken together, these results may suggest that the E/C muscle ratio may be useful to globally evaluate muscle trophism and reinnervation, but is less informative to detect specific differences among the groups (Vleggeert-Lankamp, 2007).

Extensive morphological analysis of the regenerated distal nerves showed the distinct effect of cells or autograft repair on multiple parameters such as axonal and fiber diameters and myelinated surfaces. We found that g-ratio values (AD/FD) were close to optimal and did not vary among the groups, as a further proof of structurally and functionally correct axonal myelination, independently from single groups features (Chomiak and Hu, 2009). Taken together, all these results confirmed the favourable effect of primary SC, in term of myelination of regenerating fibers, myelinated surface, prevention of muscle atrophy and improvement of fiber diameter, consistent with previous literature. SC-like differentiated MSC, even if displaying a significant improvement in gastrocnemius muscle mass after total axotomy, showed a weaker regenerative potential when compared to SC-like ASC, which closely approached the results of the autograft group in both morphological and functional evaluations. Even if in a previous *in vivo* experiment (di Summa et al., 2010), dMSC and dASC showed overlapping results, in this long term study dMSC did not achieve such dASC positive effects on regeneration. The significantly higher fiber density registered in the dMSC group may explain this difference as it could be a sign of axonal branching (Vleggeert-Lankamp, 2007) which leads to less efficient nerve conductivity and function (Ijkema-Paassen et al., 2002) and may be interpreted as the morphological features of a less mature nerve, where motor axons collaterals, even if supporting muscle mass, have not been pruned to “fine tune” the motor unit (Brown and Booth, 1983; Brushart, 1993).

Although these experiments seem to provide good evidence for the benefit of regenerative cells, in particular dASC, in promoting axonal regeneration, relevant issues need to be addressed further. It has been previously shown that cell survival within tube grafts may be poor in the long term (Heine et al., 2004; Marchesi et al., 2007).

This may lead to the question whether the growth promoting effect should be addressed to the originally transplanted cell population or to an indirect effect of the endogenous cell population, or both. Moreover, it is still difficult to explain exactly how these cells are exerting their effect. Predifferentiating of stem cells to a Schwann cell phenotype has been shown to remarkably improve survival of the stem cells (McKenzie et al., 2006). This may be due to the fact that mature Schwann cells survive denervation events by secreting autocrine factors such as insulin-like growth factor and neurotrophin 3 (Jessen and Mirsky, 1999), which lead to self preservation and supplying of the injured nerve. Consequently, Schwann cell-like differentiation could improve survival and effectiveness of transplanted stem cells. However, when quantified, precursor cells have shown a survival rate between 0.5% and 38%, depending on evaluation time point and cell type (Walsh and Midha, 2009). If considering that improvement in regeneration outcomes has been also observed in the absence or with minimal detection of transplanted cells (Pan et al., 2007) a direct or indirect stimulation of resident glial cells may be involved. It has been recently hypothesized how transplanted adult bone marrow stem cells may indirectly improve regeneration of motor and sensory axons after sciatic nerve injury. Although the transplanted cells did not show evidence of differentiation into Schwann cells *in situ*, their presence dramatically increased the number of macrophages, accelerating debris removal and increasing the concentration of inflammatory, growth promoting and trophic factors (Ribeiro-Resende et al., 2009). This suggests that cells are supporting axonal growth by additional mechanisms such as production of cytokines and neurotrophic factors or harnessing the inflammatory response (Murakami et al., 2003), which lead to the proliferation of host Schwann and satellite cells. In this sense, the presence of transplanted cells seems to be more crucial in the early phase after injury to trigger the regeneration process and boost the endogenous cell populations. Further, in spinal cord injuries, adipose tissue stromal cells have been shown to prevent apoptosis-mediated neuronal death and hypomyelination by acting on macrophage and glial cell infiltration at the site of injury (Kang et al., 2007). The neuroprotective properties of dASC may be one possible mechanism of the improved regeneration we noticed in the present experiment, as it seems to be consistent with the higher number of retrograde labelled motoneurons when compared to other experimental groups.

## CONCLUSION

In conclusion, SC-like differentiated adipose-derived stem cells confirmed in this long term *in vivo* experiment the neurotrophic potential expressed *in vitro*, closely following or even matching morphological and functional results of the autografts, the actual gold standard in clinical practice. These results suggest that SC-like differentiated ASC, may substitute SC and are likely to be one of the most clinically translatable cell types to be employed in nerve regeneration.

**Acknowledgments**—We are grateful to Prof Daniel Egloff for the excellent administrative support and to Dr. Dominique Schaakxs and Patricia Engels (Department of Plastic Surgery, Centre Hospitalier Universitaire Vaudois, Lausanne, Switzerland) for help and assistance in animal experimental procedures and tissue processing. We are thankful to Prof. Damien Debatisse (Department of Neurosurgery, Universität Kliniken der Stadt, Köln, Germany) for advice about the neurophysiology procedures and Dr Lev Novikov and Dr Liudmila Novikova for helpful discussions on retrograde labelling. We want to finally thank Federico Turatti (Politecnico di Torino, Turin, Italy) for his useful advices and help in data handling and analysis. The authors are grateful to the Swiss National Fund (Fonds National Suisse de la Recherche Scientifique) for the scholarship which supported the work of P.G. di Summa, and to the SwissLife Foundation, the SUVA and the University of Lausanne FBM for their financial support to the project.

## REFERENCES

- Ashjian PH, Elbarbary AS, Edmonds B, DeUgarte D, Zhu M, Zuk PA, Lorenz HP, Benhaim P, Hedrick MH (2003) *In vitro* differentiation of human processed lipoaspirate cells into early neural progenitors. *Plast Reconstr Surg* 111:1922–1931.
- Barry FP, Murphy JM (2004) Mesenchymal stem cells: clinical applications and biological characterization. *Int J Biochem Cell Biol* 36:568–584.
- Belkas JS, Shoichet MS, Midha R (2004) Peripheral nerve regeneration through guidance tubes. *Neurol Res* 26:151–160.
- Bensaid W, Triffitt JT, Blanchat C, Oudina K, Sedel L, Petite H (2003) A biodegradable fibrin scaffold for mesenchymal stem cell transplantation. *Biomaterials* 24:2497–2502.
- Brown MC, Booth CM (1983) Postnatal development of the adult pattern of motor axon distribution in rat muscle. *Nature* 304:741–742.
- Brushart TM (1993) Motor axons preferentially reinnervate motor pathways. *J Neurosci* 13:2730–2738.
- Caddick J, Kingham PJ, Gardiner NJ, Wiberg M, Terenghi G (2006) Phenotypic and functional characteristics of mesenchymal stem cells differentiated along a Schwann cell lineage. *Glia* 54:840–849.
- Chalfoun CT, Wirth GA, Evans GR (2006) Tissue engineered nerve constructs: where do we stand? *J Cell Mol Med* 10:309–317.
- Chen ZL, Yu WM, Strickland S (2007) Peripheral regeneration. *Annu Rev Neurosci* 30:209–233.
- Chomiak T, Hu B (2009) What is the optimal value of the g-ratio for myelinated fibers in the rat CNS? A theoretical approach. *PLoS One* 4:e7754.
- Dezawa M, Takahashi I, Esaki M, Takano M, Sawada H (2001) Sciatic nerve regeneration in rats induced by transplantation of *in vitro* differentiated bone-marrow stromal cells. *Eur J Neurosci* 14:1771–1776.
- Di Scipio F, Raimondo S, Tos P, Geuna S (2008) A simple protocol for paraffin-embedded myelin sheath staining with osmium tetroxide for light microscope observation. *Microsc Res Tech* 71:497–502.
- di Summa PG, Kingham PJ, Raffoul W, Wiberg M, Terenghi G, Kalbermatten DF (2010) Adipose-derived stem cells enhance peripheral nerve regeneration. *J Plast Reconstr Aesthet Surg* 63:1544–1552.
- Erba P, Terenghi G, Kingham PJ (2010) Neural differentiation and therapeutic potential of adipose tissue derived stem cells. *Curr Stem Cell Res Ther* 5:153–160.
- Fine EG, Decosterd I, Papalozos M, Zurn AD, Aebischer P (2002) GDNF and NGF released by synthetic guidance channels support sciatic nerve regeneration across a long gap. *Eur J Neurosci* 15:589–601.
- Gardner RL (2007) Stem cells and regenerative medicine: principles, prospects and problems. *C R Biol* 330:465–473.

- Guenard V, Kleitman N, Morrissey TK, Bunge RP, Aebischer P (1992) Syngeneic Schwann cells derived from adult nerves seeded in semipermeable guidance channels enhance peripheral nerve regeneration. *J Neurosci* 12:3310–3320.
- Guilak F, Lott KE, Awad HA, Cao Q, Hicok KC, Fermor B, Gimble JM (2006) Clonal analysis of the differentiation potential of human adipose-derived adult stem cells. *J Cell Physiol* 206:229–237.
- Hall S (1997) Axonal regeneration through acellular muscle grafts. *J Anat* 190 (Pt 1):57–71.
- Heine W, Conant K, Griffin JW, Hoke A (2004) Transplanted neural stem cells promote axonal regeneration through chronically denervated peripheral nerves. *Exp Neurol* 189:231–240.
- Ide C (1996) Peripheral nerve regeneration. *Neurosci Res* 25:101–121.
- Ijkema-Paassen J, Meek MF, Gramsbergen A (2002) Reinnervation of muscles after transection of the sciatic nerve in adult rats. *Muscle Nerve* 25:891–897.
- Jacob JM (1998) Lumbar motor neuron size and number is affected by age in male F344 rats. *Mech Ageing Dev* 106:205–216.
- Jessen KR, Mirsky R (1999) Why do Schwann cells survive in the absence of axons? *Ann N Y Acad Sci* 883:109–115.
- Johnsen B, Fuglsang-Frederiksen A (2000) Electrodiagnosis of polyneuropathy. *Neurophysiol Clin* 30:339–351.
- Jubran M, Widenfalk J (2003) Repair of peripheral nerve transections with fibrin sealant containing neurotrophic factors. *Exp Neurol* 181:204–212.
- Kalbermatten DF, Kingham PJ, Mahay D, Mantovani C, Pettersson J, Raffoul W, Balcin H, Pierer G, Terenghi G (2008) Fibrin matrix for suspension of regenerative cells in an artificial nerve conduit. *J Plast Reconstr Aesthet Surg* 61:669–675.
- Kalbermatten DF, Pettersson J, Kingham PJ, Pierer G, Wiberg M, Terenghi G (2009) New fibrin conduit for peripheral nerve repair. *J Reconstr Microsurg* 25:27–33.
- Kang SK, Putnam LA, Ylostalo J, Popescu IR, Dufour J, Belousov A, Bunnell BA (2004) Neurogenesis of rhesus adipose stromal cells. *J Cell Sci* 117:4289–4299.
- Kang SK, Yeo JE, Kang KS, Phinney DG (2007) Cytoplasmic extracts from adipose tissue stromal cells alleviates secondary damage by modulating apoptosis and promotes functional recovery following spinal cord injury. *Brain Pathol* 17:263–275.
- Keilhoff G, Gohl A, Langnase K, Fansa H, Wolf G (2006) Transdifferentiation of mesenchymal stem cells into Schwann cell-like myelinating cells. *Eur J Cell Biol* 85:11–24.
- Kingham PJ, Kalbermatten DF, Mahay D, Armstrong SJ, Wiberg M, Terenghi G (2007) Adipose-derived stem cells differentiate into a Schwann cell phenotype and promote neurite outgrowth *in vitro*. *Exp Neurol* 207:267–274.
- Kokai LE, Rubin JP, Marra KG (2005) The potential of adipose-derived adult stem cells as a source of neuronal progenitor cells. *Plast Reconstr Surg* 116:1453–1460.
- Mantovani C, Mahay D, Kingham PJ, Terenghi G, Shawcross SG, Wiberg M (2010) Bone marrow- and adipose-derived stem cells show expression of myelin mRNAs and proteins. *Regen Med* 5:403–410.
- Marchesi C, Pluderer M, Colleoni F, Belicchi M, Merigalli M, Farini A, Parolini D, Draghi L, Fruguglietti ME, Gavina M, Porretti L, Cattaneo A, Battistelli M, Prella A, Moggio M, Borsa S, Bello L, Spagnoli D, Gaini SM, Tanzi MC, Bresolin N, Grimoldi N, Torrente Y (2007) Skin-derived stem cells transplanted into resorbable guides provide functional nerve regeneration after sciatic nerve resection. *Glia* 55:425–438.
- Matsumoto T, Kano K, Kondo D, Fukuda N, Iribe Y, Tanaka N, Matsumura Y, Sakuma T, Satomi A, Otaki M, Ryu J, Mugishima H (2008) Mature adipocyte-derived dedifferentiated fat cells exhibit multilineage potential. *J Cell Physiol* 215:210–222.
- McKenzie IA, Biernaskie J, Toma JG, Midha R, Miller FD (2006) Skin-derived precursors generate myelinating Schwann cells for the injured and dysmyelinated nervous system. *J Neurosci* 26:6651–6660.
- Mirsky R, Jessen KR, Brennan A, Parkinson D, Dong Z, Meier C, Parmantier E, Lawson D (2002) Schwann cells as regulators of nerve development. *J Physiol Paris* 96:17–24.
- Mohanna PN, Terenghi G, Wiberg M (2005) Composite PHB-GGF conduit for long nerve gap repair: a long-term evaluation. *Scand J Plast Reconstr Surg Hand Surg* 39:129–137.
- Mosahebi A, Woodward B, Wiberg M, Martin R, Terenghi G (2001) Retroviral labeling of Schwann cells: *in vitro* characterization and *in vivo* transplantation to improve peripheral nerve regeneration. *Glia* 34:8–17.
- Murakami T, Fujimoto Y, Yasunaga Y, Ishida O, Tanaka N, Ikuta Y, Ochi M (2003) Transplanted neuronal progenitor cells in a peripheral nerve gap promote nerve repair. *Brain Res* 974:17–24.
- Pan HC, Cheng FC, Chen CJ, Lai SZ, Lee CW, Yang DY, Chang MH, Ho SP (2007) Post-injury regeneration in rat sciatic nerve facilitated by neurotrophic factors secreted by amniotic fluid mesenchymal stem cells. *J Clin Neurosci* 14:1089–1098.
- Pereira Lopes FR, Camargo de Moura Campos L, Dias Correa J Jr, Balduino A, Lora S, Langone F, Borojevic R, Blanco Martinez AM (2006) Bone marrow stromal cells and resorbable collagen guidance tubes enhance sciatic nerve regeneration in mice. *Exp Neurol* 198:457–468.
- Pettersson J, Kalbermatten D, McGrath A, Novikova LN (2010) Biodegradable fibrin conduit promotes long-term regeneration after peripheral nerve injury in adult rats. *J Plast Reconstr Aesthet Surg* 63:1893–1899.
- Pfister LA, Papaloizos M, Merkle HP, Gander B (2007) Nerve conduits and growth factor delivery in peripheral nerve repair. *J Peripher Nerv Syst* 12:65–82.
- Piquilloud G, Christen T, Pfister LA, Gander B, Papaloizos MY (2007) Variations in glial cell line-derived neurotrophic factor release from biodegradable nerve conduits modify the rate of functional motor recovery after rat primary nerve repairs. *Eur J Neurosci* 26:1109–1117.
- Ribeiro-Resende VT, Pimentel-Coelho PM, Mesentier-Louro LA, Mendez RM, Mello-Silva JP, Cabral-da-Silva MC, de Mello FG, de Melo Reis RA, Mendez-Otero R (2009) Trophic activity derived from bone marrow mononuclear cells increases peripheral nerve regeneration by acting on both neuronal and glial cell populations. *Neuroscience* 159:540–549.
- Rodriguez AM, Pisani D, Dechesne CA, Turc-Carel C, Kurzenne JY, Wdziekonski B, Villageois A, Bagnis C, Breittmayer JP, Groux H, Ailhaud G, Dani C (2005) Transplantation of a multipotent cell population from human adipose tissue induces dystrophin expression in the immunocompetent mdx mouse. *J Exp Med* 201:1397–1405.
- Rodriguez FJ, Verdu E, Ceballos D, Navarro X (2000) Nerve guides seeded with autologous Schwann cells improve nerve regeneration. *Exp Neurol* 161:571–584.
- Safford KM, Hicok KC, Safford SD, Halvorsen YD, Wilkison WO, Gimble JM, Rice HE (2002) Neurogenic differentiation of murine and human adipose-derived stromal cells. *Biochem Biophys Res Commun* 294:371–379.
- Safford KM, Safford SD, Gimble JM, Shetty AK, Rice HE (2004) Characterization of neuronal/glial differentiation of murine adipose-derived adult stromal cells. *Exp Neurol* 187:319–328.
- Sanchez-Ramos J, Song S, Cardozo-Pelaez F, Hazzi C, Stedeford T, Willing A, Freeman TB, Saporta S, Janssen W, Patel N, Cooper DR, Sanberg PR (2000) Adult bone marrow stromal cells differentiate into neural cells *in vitro*. *Exp Neurol* 164:247–256.
- Santiago LY, Clavijo-Alvarez J, Brayfield C, Rubin JP, Marra KG (2009) Delivery of adipose-derived precursor cells for peripheral nerve repair. *Cell Transplant* 18:145–158.
- Strem BM, Hicok KC, Zhu M, Wulur I, Alfonso Z, Schreiber RE, Fraser JK, Hedrick MH (2005) Multipotential differentiation of adipose tissue-derived stem cells. *Keio J Med* 54:132–141.

- Tankisi H, Pugdahl K, Johnsen B, Fuglsang-Frederiksen A (2007) Correlations of nerve conduction measures in axonal and demyelinating polyneuropathies. *Clin Neurophysiol* 118:2383–2392.
- Taylor CA, Braza D, Rice JB, Dillingham T (2008) The incidence of peripheral nerve injury in extremity trauma. *Am J Phys Med Rehabil* 87:381–385.
- Terenghi G (1995) Peripheral nerve injury and regeneration. *Histol Histopathol* 10:709–718.
- Tholpady SS, Katz AJ, Ogle RC (2003) Mesenchymal stem cells from rat visceral fat exhibit multipotential differentiation *in vitro*. *Anat Rec A Discov Mol Cell Evol Biol* 272:398–402.
- Tohill M, Mantovani C, Wiberg M, Terenghi G (2004a) Rat bone marrow mesenchymal stem cells express glial markers and stimulate nerve regeneration. *Neurosci Lett* 362:200–203.
- Tohill MP, Mann DJ, Mantovani CM, Wiberg M, Terenghi G (2004b) Green fluorescent protein is a stable morphological marker for Schwann cell transplants in bioengineered nerve conduits. *Tissue Eng* 10:1359–1367.
- Vleggeert-Lankamp CL (2007) The role of evaluation methods in the assessment of peripheral nerve regeneration through synthetic conduits: a systematic review. Laboratory investigation. *J Neurosurg* 107:1168–1189.
- Walsh S, Midha R (2009) Practical considerations concerning the use of stem cells for peripheral nerve repair. *Neurosurg Focus* 26:E2.
- Wang G, Lu G, Ao Q, Gong Y, Zhang X (2010) Preparation of cross-linked carboxymethyl chitosan for repairing sciatic nerve injury in rats. *Biotechnol Lett* 32:59–66.
- Whitlock EL, Tuffaha SH, Luciano JP, Yan Y, Hunter DA, Magill CK, Moore AM, Tong AY, Mackinnon SE, Borschel GH (2009) Processed allografts and type I collagen conduits for repair of peripheral nerve gaps. *Muscle Nerve* 39:787–799.
- Zhang Y, Luo H, Zhang Z, Lu Y, Huang X, Yang L, Xu J, Yang W, Fan X, Du B, Gao P, Hu G, Jin Y (2010) A nerve graft constructed with xenogeneic acellular nerve matrix and autologous adipose-derived mesenchymal stem cells. *Biomaterials* 31:5312–5324.
- Zuk PA, Zhu M, Ashjian P, De Ugarte DA, Huang JI, Mizuno H, Alfonso ZC, Fraser JK, Benhaim P, Hedrick MH (2002) Human adipose tissue is a source of multipotent stem cells. *Mol Biol Cell* 13:4279–4295.
- Zuk PA, Zhu M, Mizuno H, Huang J, Futrell JW, Katz AJ, Benhaim P, Lorenz HP, Hedrick MH (2001) Multilineage cells from human adipose tissue: implications for cell-based therapies. *Tissue Eng* 7:211–228.

(Accepted 21 February 2011)